

See discussions, stats, and author profiles for this publication at: <https://www.researchgate.net/publication/23182296>

# H(2), HD, and D(2) inside C(60): Coupled translation-rotation eigenstates of the endohedral molecules from quantum five-dimensional calculations

Article in The Journal of Chemical Physics · September 2008

DOI: 10.1063/1.2967858 · Source: PubMed

CITATIONS

84

READS

306

5 authors, including:



Francesco Sebastianelli

Sapienza University of Rome

7 PUBLICATIONS 173 CITATIONS

SEE PROFILE



Ronald G Lawler

Brown University

140 PUBLICATIONS 4,270 CITATIONS

SEE PROFILE

# H<sub>2</sub>, HD, and D<sub>2</sub> inside C<sub>60</sub>: Coupled translation-rotation eigenstates of the endohedral molecules from quantum five-dimensional calculations

Minzhong Xu,<sup>1</sup> Francesco Sebastianelli,<sup>1</sup> Zlatko Bačić,<sup>1,a)</sup> Ronald Lawler,<sup>2</sup> and Nicholas J. Turro<sup>3,b)</sup>

<sup>1</sup>Department of Chemistry, New York University, New York, New York 10003, USA

<sup>2</sup>Department of Chemistry, Brown University, Providence, Rhode Island 02912, USA

<sup>3</sup>Department of Chemistry, Columbia University, New York, New York 10027, USA

(Received 27 May 2008; accepted 14 July 2008; published online 13 August 2008)

We have performed rigorous quantum five-dimensional (5D) calculations of the translation-rotation (T-R) energy levels and wave functions of H<sub>2</sub>, HD, and D<sub>2</sub> inside C<sub>60</sub>. This work is an extension of our earlier investigation of the quantum T-R dynamics of H<sub>2</sub>@C<sub>60</sub> [M. Xu *et al.*, J. Chem. Phys. **128**, 011101 (2008)] and uses the same computational methodology. Two 5D intermolecular potential energy surfaces (PESs) were employed, differing considerably in their well depths and the degree of confinement of the hydrogen molecule. Our calculations revealed pronounced sensitivity of the endohedral T-R dynamics to the differences in the interaction potentials, and to the large variations in the masses and the rotational constants of H<sub>2</sub>, HD, and D<sub>2</sub>. The T-R levels vary significantly in their energies and ordering on the two PESs, as well as from one isotopomer to another. Nevertheless, they all display the same distinctive patterns of degeneracies, which can be qualitatively understood and assigned in terms of the model which combines the isotropic three-dimensional harmonic oscillator, the rigid rotor, and the coupling between the orbital and the rotational angular momenta of H<sub>2</sub>/HD/D<sub>2</sub>. The quantum number  $j$  associated with the rotation of H<sub>2</sub>, HD, and D<sub>2</sub> was found to be a good quantum number for H<sub>2</sub> and D<sub>2</sub> on both PESs, while most of the T-R levels of HD exhibit strong mixing of two or more rotational basis functions with different  $j$  values. © 2008 American Institute of Physics. [DOI: 10.1063/1.2967858]

## I. INTRODUCTION

Among the many intriguing properties of C<sub>60</sub> and other fullerenes, one that has particularly fascinated experimental synthetic and physical chemists, as well as theoretical chemists, is the possibility of encapsulating atoms and molecules inside the fullerene cavities and investigating their physical and chemical properties. The endohedral H<sub>2</sub>-C<sub>60</sub> complex, denoted H<sub>2</sub>@C<sub>60</sub>, has received a great deal of attention, not only as the endohedral complex involving the simplest molecule but also the most highly quantum mechanical. H<sub>2</sub>@C<sub>60</sub> can now be synthesized<sup>1,2</sup> in quantities exceeding 100 mg using the “molecular surgery” approach,<sup>3</sup> where in a series of organic reactions an orifice is opened in the cage of C<sub>60</sub>, H<sub>2</sub> molecule is inserted through the orifice, which is then closed leaving H<sub>2</sub> trapped inside. The availability of H<sub>2</sub>@C<sub>60</sub> in macroscopic amounts has enabled the investigations of the dynamical properties of the endohedral H<sub>2</sub> in C<sub>60</sub> and related fullerenes using NMR spectroscopy,<sup>4–6</sup> as well as of its ability to quench the external singlet molecular oxygen.<sup>7</sup>

The three translational degrees of freedom of H<sub>2</sub> inside C<sub>60</sub> are quantized as a result of the confinement, in addition to the quantization of its two rotational degrees of freedom. H<sub>2</sub>, HD, and D<sub>2</sub> are light molecules with large rotational

constants, 59.3, 44.7, and 29.9 cm<sup>-1</sup>, respectively. Encapsulating them inside the fullerene, whose cavity accessible to the endohedral molecule has the diameter of 3–4 a.u. (see Fig. 1), gives rise to a rather sparse set of translation-rotation (T-R) eigenstates well separated in energy. As a result, the dynamics of the translational and rotational “rattling” motions of H<sub>2</sub>/HD/D<sub>2</sub> in C<sub>60</sub> is highly quantum mechanical. The intrinsically quantum nature of this system is enhanced further by the fact that, due to the symmetry requirements of the total wave function, the homonuclear isotopomers H<sub>2</sub> and D<sub>2</sub> appear in two distinct species, having either only even- $j$  rotational states, parahydrogen ( $p$ -H<sub>2</sub>) and orthodeuterium ( $o$ -D<sub>2</sub>), or exclusively odd- $j$  rotational states, orthohydrogen ( $o$ -H<sub>2</sub>) and paradeuterium ( $p$ -D<sub>2</sub>). Therefore, H<sub>2</sub>/HD/D<sub>2</sub>@C<sub>60</sub> provides a paradigm of the quantum T-R dynamics of a light molecule in a confined geometry with high symmetry, one which is amenable to high-level experimental and theoretical investigations.

In a recent paper<sup>8</sup> (paper I), we reported the first quantum five-dimensional calculations of the T-R energy levels and wave functions of a hydrogen molecule,  $p$ - and  $o$ -H<sub>2</sub>, inside C<sub>60</sub>. The three translational and the two rotational degrees of freedom of the endohedral H<sub>2</sub> were treated rigorously, as fully coupled, while the C<sub>60</sub> cage and H<sub>2</sub> were taken to be rigid. This study revealed that the calculated T-R level structure, exhibiting an intricate pattern of degeneracies, can be fully understood in terms of a few salient features, which

<sup>a)</sup>Electronic mail: zlatko.bacic@nyu.edu.

<sup>b)</sup>Electronic mail: njt3@columbia.edu.

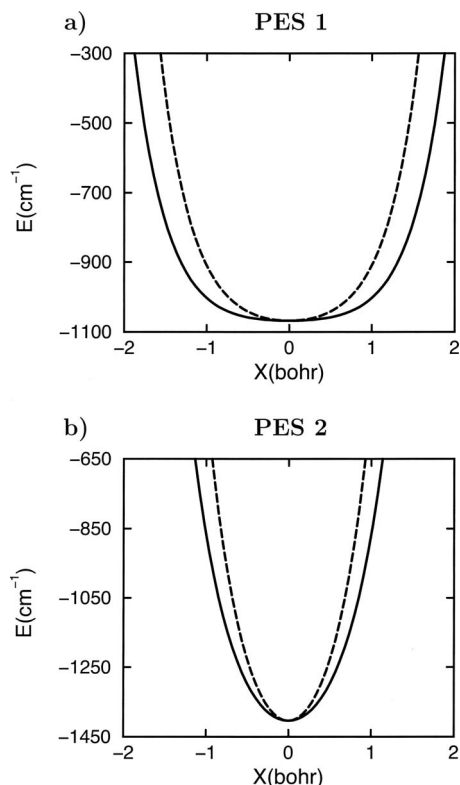


FIG. 1. One-dimensional cuts through the 5D interaction potentials (a) PES 1 and (b) PES 2 of  $H_2$  inside  $C_{60}$  along a  $C_2$  axis of  $C_{60}$ , for  $H_2$  perpendicular (full line) and parallel (dashed line) to the axis.

include the coupling between the orbital and the rotational angular momenta of  $H_2$  to give the total angular momentum  $\lambda$ , and the splitting of the sevenfold degeneracy of the  $\lambda=3$  levels by the icosahedral  $I_h$  environment of  $C_{60}$ , in accordance with the group theory considerations.<sup>9</sup>

In this paper, our investigations of the quantum T-R dynamics of endohedral molecules are extended beyond  $H_2$  to include also  $D_2$  and  $HD$  in  $C_{60}$ , using the methodology of paper I. The masses and the rotational constants of  $H_2$ ,  $HD$ , and  $D_2$  differ substantially, and it is of interest to explore how these differences affect the T-R dynamics in the highly quantum regime. Furthermore, the T-R energy levels of all three isotopomers are calculated on two different five-dimensional (5D) intermolecular potential energy surfaces of  $H_2@C_{60}$ , in order to examine the sensitivity of the T-R level structure to the properties of the interaction potentials.

## II. THEORY

The computational methodology employed in this work was described in paper I. It was developed by us earlier for the purpose of calculating the T-R eigenstates of  $H_2$  and isotopomers inside the cages of the clathrate hydrates.<sup>10–13</sup>  $C_{60}$  is treated as rigid, and the geometry used in our calculations, which has the icosahedral ( $I_h$ ) symmetry, is virtually identical to the experimental one.<sup>14</sup> The bond length of the endohedral molecule is also held fixed. The set of five coordinates  $(x, y, z, \theta, \phi)$  is employed;  $x$ ,  $y$  and  $z$  are the Cartesian coordinates of the center of mass (cm) of  $H_2/HD/D_2$ , while the two polar angles  $\theta$  and  $\phi$  specify its orientation. The coordinate system is aligned with three orthogonal  $C_2$  axes of  $C_{60}$ ,

and its origin is at the cm of the cage. Alternatively, the position of the cm of the guest diatomic could be defined using a set of spherical polar coordinates  $(|\mathbf{R}|, \Theta, \Phi)$ , where  $|\mathbf{R}|$  is the length of the vector  $\mathbf{R}$  connecting of the cm of the molecule and the center of the cage, while  $\Theta$  and  $\Phi$  are its polar angles. They were used, for example, in the bound-state calculations of  $CO@C_{60}$ .<sup>15</sup> Given that the shape of  $C_{60}$  is close to spherical, these coordinates would work well computationally and might even offer some advantages in the analysis of the results. However, our intention was to formulate a general approach that would be applicable to molecules confined in cages with fairly arbitrary, nonspherical geometries, in which case the Cartesian coordinates  $(x, y, z)$  are much more appropriate.

The rotational constants of  $C_{60}$ , a spherical top, are only  $0.0028 \text{ cm}^{-1}$ ,<sup>15</sup> and therefore the fullerene can be treated as nonrotating. Then, the 5D Hamiltonian for the T-R motions of the trapped  $H_2$  molecule is

$$H = -\frac{\hbar^2}{2\mu} \left( \frac{\partial^2}{\partial x^2} + \frac{\partial^2}{\partial y^2} + \frac{\partial^2}{\partial z^2} \right) + B\mathbf{j}^2 + V(x, y, z, \theta, \phi). \quad (1)$$

In Eq. (1),  $\mu$  is the reduced mass of  $H_2/HD/D_2@C_{60}$  and  $\mathbf{j}^2$  is the angular momentum operator of the diatomic. The mass of the guest molecule could have been used instead of  $\mu$ , since the two differ by just 0.30% for  $H_2$  and 0.55% for  $D_2$ ; the results would remain practically the same.  $B$  denotes the rotational constant of the endohedral molecule:  $B_{H_2} = 59.322 \text{ cm}^{-1}$ ,  $B_{HD} = 44.662 \text{ cm}^{-1}$ , and  $B_{D_2} = 29.904 \text{ cm}^{-1}$ .  $V(x, y, z, \theta, \phi)$  in Eq. (1) is the 5D potential energy surface (PES) described below. The energy levels and wave functions of the Hamiltonian in Eq. (1) are obtained utilizing the efficient computational methodology whose detailed description is available.<sup>10,16</sup> The final Hamiltonian matrix, its size drastically reduced by the sequential diagonalization and truncation procedure,<sup>17</sup> is diagonalized yielding the T-R eigenstates which are numerically exact for the 5D PES employed.

It was pointed out in paper I that the  $H_2$ -fullerene interactions, which are primarily dispersive, would be prohibitively time consuming to calculate accurately using high-level *ab initio* electronic structure methods. Therefore, following the theoretical investigations of  $H_2$  in single-walled carbon nanotubes<sup>18,19</sup> and on graphite,<sup>20</sup> the intermolecular 5D PES for  $H_2$  inside  $C_{60}$  was constructed as a sum over the pairwise interaction of each H atom of  $H_2$  with each C atom of  $C_{60}$ . The two-body H-C interaction was modeled with the Lennard-Jones (LJ) 12-6 potential

$$V_{LJ}(r) = 4\epsilon_{HC} \left[ \left( \frac{\sigma_{HC}}{r} \right)^{12} - \left( \frac{\sigma_{HC}}{r} \right)^6 \right], \quad (2)$$

where  $\epsilon_{HC}$  is the well depth of the potential and  $\sigma_{HC}$  is related to its equilibrium distance  $r_e$ , as  $r_e = 2^{1/6}\sigma_{HC}$ . In paper I, the set of LJ parameters referred to in Ref. 18 as FB,<sup>19</sup> in which  $\epsilon_{HC} = 19.2 \text{ cm}^{-1}$  and  $\sigma_{HC} = 3.08 \text{ \AA}$ , was employed. They generate a 5D PES for  $H_2@C_{60}$ , with the well depth of  $-1403.87 \text{ cm}^{-1}$ . This PES is used also in the present work and is designated here as PES 2. In addition, the second intermolecular 5D PES is used, designated as PES 1. It is

TABLE I. Translation-rotation (T-R) energy levels of *p*-H<sub>2</sub> inside C<sub>60</sub>, from the quantum 5D calculations on PES 1 and PES 2 defined in the text. The excitation energies  $\Delta E$  (in cm<sup>-1</sup>) are relative to the ground-state energy  $E_0 = -1012.009$  cm<sup>-1</sup> (PES 2) and  $E_0 = 898.479$  cm<sup>-1</sup> (PES 1);  $g$  denotes the degeneracy of the levels.  $n$  and  $l$  are the principal and the orbital angular momentum quantum numbers, respectively, of the 3D isotropic harmonic oscillator,  $j$  is the quantum number of the dominant H<sub>2</sub> rotational basis function, and  $c(j)$  is its contribution to a T-R eigenstate;  $\lambda$  is the quantum number of the total angular momentum operator  $\lambda = \mathbf{j} + \mathbf{l}$ . The values of  $l$  shown are those allowed for the given  $n$ .  $\langle R \rangle$  (in a.u.) is the mean value of the distance between the centers of mass of H<sub>2</sub> and C<sub>60</sub>.

$n$	$j$	$l$	$\lambda$	$g$	PES 2			PES 1		
					$\Delta E$	$c(j)$	$\langle R \rangle$	$\Delta E$	$c(j)$	$\langle R \rangle$
0	0	0	0	1	0.00	0.998	0.57	0.00	0.998	0.81
1	0	1	1	3	279.47	0.990	0.71	136.68	0.995	0.99
0	2	0	2	5	354.92	0.994	0.57	357.68	0.975	0.81
2	0	0,2	2	5	574.52	0.975	0.82	287.26	0.965	1.12
2	0	0,2	0	1	593.27	0.968	0.81	316.16	0.983	1.07
1	2	1	2	5	615.58	0.999	0.72	479.22	0.999	1.01
1	2	1	3	4	640.02	0.984	0.72	503.99	0.879	1.01
1	2	1	3	3	640.36	0.983	0.72	505.20	0.867	1.01
1	2	1	1	3	662.28	0.985	0.70	519.95	0.704	1.02
3	0	1,3	3	4	883.64	0.956	0.91	447.98	0.864	1.21
3	0	1,3	3	3	883.97	0.954	0.91	447.73	0.852	1.21
3	0	1,3	1	3	914.13	0.944	0.90	486.25	0.680	1.12

defined by the set of LJ parameters which Ref. 18 referred to as NW,<sup>20</sup> where  $\epsilon_{\text{HC}} = 18.0$  cm<sup>-1</sup> and  $\sigma_{\text{HC}} = 2.78$  Å. The well depth of PES 1,  $-1068.11$  cm<sup>-1</sup>, is much smaller than that of PES 2. Figure 1 shows the one-dimensional (1D) cuts of both PES 1 and PES 2 along a C<sub>2</sub> axis of C<sub>60</sub>. They reveal that the two PESs differ substantially not only by how deep they are but also by their shapes and the cavity sizes they provide for the endohedral H<sub>2</sub>. The 1D cuts are displayed for H<sub>2</sub> perpendicular and parallel to the fullerene axis, in order to show the anisotropy of the interaction potential with respect to the angular orientation of the H<sub>2</sub> molecule. If the two cuts were to coincide, then H<sub>2</sub> inside C<sub>60</sub> would effectively behave as a structureless, spherical particle. It is clear from Fig. 1 that this is not the case.

In our computational method, the basis set is defined by the following main parameters:  $M$ , the dimension of the sine discrete variable representation (DVR) for each of the three Cartesian coordinates,  $d$ , the range (from  $-d$  to  $d$ ) spanned by the DVR,  $E_{\text{cut}}$ , the energy cutoff parameter for the intermediate 3D eigenvector basis,<sup>16</sup> and  $N$ , the dimension of the final full 5D Hamiltonian matrix. In the calculations reported here, the values of these parameters were as follows: (i) H<sub>2</sub> (PES 1):  $M=15$ ,  $d=2.83$  bohrs,  $E_{\text{cut}}=4000$  cm<sup>-1</sup>,  $N=39\,156$ ; (ii) H<sub>2</sub> (PES 2):  $M=15$ ,  $d=2.83$  bohrs,  $E_{\text{cut}}=5000$  cm<sup>-1</sup>,  $N=20\,264$ ; (iii) HD (PES 1):  $M=15$ ,  $d=2.83$  bohrs,  $E_{\text{cut}}=3000$  cm<sup>-1</sup>,  $N=35\,355$ ; (iv) HD (PES 2):  $M=21$ ,  $d=3.40$  bohrs,  $E_{\text{cut}}=5000$  cm<sup>-1</sup>,  $N=38\,057$ ; (v) D<sub>2</sub> (PES 1):  $M=15$ ,  $d=2.83$  bohrs,  $E_{\text{cut}}=3000$  cm<sup>-1</sup>,  $N=40\,000$ ; (vi) D<sub>2</sub> (PES 2):  $M=20$ ,  $d=3.78$  bohrs,  $E_{\text{cut}}=4000$  cm<sup>-1</sup>,  $N=23\,430$ . In all calculations, the angular basis included functions up to  $j_{\text{max}}=7$ . All basis set parameters were extensively tested for convergence, assuring that the T-R energy levels discussed in the following section are converged to five significant figures or better.

### III. RESULTS AND DISCUSSION

The T-R energy levels from the quantum 5D calculations on PESs 1 and 2 are shown for *p*-H<sub>2</sub>@C<sub>60</sub> in Table I and

Fig. 2, and for *o*-H<sub>2</sub>@C<sub>60</sub> in Table II and Fig. 3, together with their degeneracies  $g$ . The T-R levels of HD@C<sub>60</sub> calculated on PESs 1 and 2 are given in Tables III and IV, respectively, as well as in Fig. 4. For *o*- and *p*-D<sub>2</sub> in C<sub>60</sub>, only the diagrams of the T-R levels computed on PESs 1 and 2 are displayed in Figs. 5 and 6. The main purpose of Figs. 2–6 is to show more clearly the relationships between the T-R levels obtained for a given isotopomer (and nuclear spin isomer, *ortho* and *para*, except for HD) on PESs 1 and 2. Figure 7 presents the diagram of the T-R energy levels of HD@C<sub>60</sub> on PES 2 listed in Table IV, together with their counterparts (i.e., levels with the same assignments) in *p*- and *o*-H<sub>2</sub>@C<sub>60</sub> and *o*- and *p*-D<sub>2</sub>@C<sub>60</sub>, also on PES 2.

By projecting the T-R eigenvectors on the rotational basis, taking the moduli squared and integrating over  $x$ ,  $y$ , and  $z$ , one can determine the contributions  $c(j)$  made by each of the rotational basis functions to the eigenstates. In the case of *p*- and *o*-H<sub>2</sub> in Tables I and II, respectively, the contribution  $c(j)$  of the single dominant rotational basis function  $j$  is shown for each T-R eigenstate. For HD in Tables III and IV,

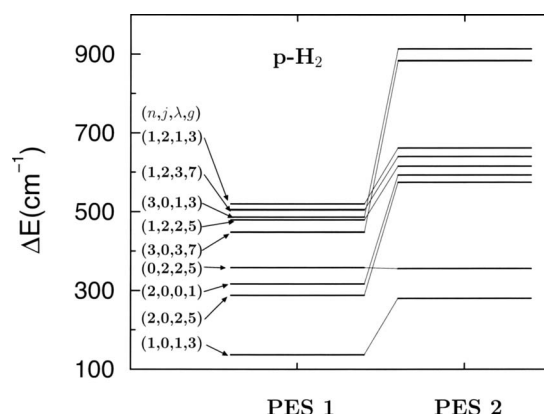


FIG. 2. Diagram of translation-rotation energy levels of *p*-H<sub>2</sub>@C<sub>60</sub> from the quantum 5D calculations on PES 1 and PES 2. The excitation energies  $\Delta E$  are relative to the ground-state energies on the two PESs. The quantum numbers  $(n, j, \lambda, g)$  are defined in the text.

TABLE II. Translation-rotation (T-R) energy levels of  $o$ -H<sub>2</sub> inside C<sub>60</sub>, from the quantum 5D calculations on PES 1 and PES 2 defined in the text. The excitation energies  $\Delta E$  (in cm<sup>-1</sup>) are relative to the ground-state energy  $E_0 = -1012.009$  cm<sup>-1</sup> (PES 2) and  $E_0 = -898.479$  cm<sup>-1</sup> (PES 1) of  $p$ -H<sub>2</sub> in C<sub>60</sub>. Other symbols have the same meaning as in Table I.

$n$	$j$	$l$	$\lambda$	$g$	PES 2			PES 1		
					$\Delta E$	$c(j)$	$\langle R \rangle$	$\Delta E$	$c(j)$	$\langle R \rangle$
0	1	0	1	3	118.45	0.999	0.57	118.31	0.999	0.81
1	1	1	1	3	378.56	0.999	0.72	242.29	0.999	1.01
1	1	1	2	5	402.73	0.996	0.71	257.64	0.998	0.99
1	1	1	0	1	445.52	0.998	0.69	284.56	0.999	0.95
2	1	0,2	2	5	665.11	0.996	0.84	389.54	0.998	1.14
2	1	0,2	1	3	683.78	0.995	0.82	408.32	0.997	1.10
2	1	0,2	3	4	686.52	0.636	0.75	411.53	0.995	1.12
2	1	0,2	3	3	687.05	0.618	0.75	413.07	0.995	1.12
0	3	0	3	4	726.79	0.643	0.66	712.37	...	...
0	3	0	3	3	727.73	0.625	0.66	712.42	...	...
2	1	0,2	1	3	765.32	0.992	0.79	460.14	0.995	1.06

not one but several largest  $c(j)$  values are given for many T-R eigenstates. Tables I–IV also list  $\langle R \rangle$ , the mean value of the distance between the centers of mass of H<sub>2</sub>/HD and C<sub>60</sub>.

### A. Quantum numbers assignment

Tables I–IV reveal that the T-R levels of H<sub>2</sub> and HD calculated on both PESs 1 and 2, as well as those of D<sub>2</sub> not shown here, all display the same conspicuous pattern of degeneracies found in paper I for  $p$ - and  $o$ -H<sub>2</sub> on what is here referred to as PES 2. In paper I, we showed that this T-R level structure could be qualitatively understood and assigned by resorting to a model which incorporates the following features:

(1) The building blocks of the model are (a) the isotropic three-dimensional (3D) harmonic oscillator (HO), suggested by the high symmetry of the C<sub>60</sub> cage, for the translational degrees of freedom of the cm of the hydrogen molecule, and (b) the rigid rotor for the rotation of H<sub>2</sub> about its cm. The energy levels of the 3D isotropic HO are labeled by the principal quantum number  $n$  and the orbital angular momentum quantum number  $l$ , whose allowed values are  $n, n-2, \dots, 1$ , or 0, for odd or even  $n$ , respectively. When the possible values

of  $m, -l \leq m \leq l$ , are taken into account, the degree of degeneracy of the energy levels of the isotropic 3D HO, denoted here  $g_n^{\text{HO}}$ , is  $\frac{1}{2}(n+1)(n+2)$ , e.g., 3 for  $n=1$ , 6 for  $n=2$ , and 10 for  $n=3$ . For the rigid rotor (RR) level with the quantum number  $j, j=0, 1, 2, \dots$ , the degeneracy  $g_j^{\text{RR}}$  is  $2j+1$ . The total number of T-R states having the same  $n$  and  $j$  is  $g_n^{\text{HO}} \times (2j+1)$ .

The assignment of the quantum number  $n$  can be made by considering the values of  $\langle R \rangle$ , the trends in the excitation energies, and inspection of the wave function plots, while  $j$  is assigned based on the contribution  $c(j)$  of the dominant rotational basis functions.

As long as the translational and rotational degrees of freedom of the endohedral molecule are viewed as separate, it is *not* possible to account for, rationalize the fact that, except for the lowest few, the T-R states which have the same values of  $n, j$  invariably appear split into two or more energy levels with different degrees of degeneracy. To explain this, in paper I, we introduced the second key feature below.

(2) The orbital angular momentum  $\mathbf{l}$  of the cm of H<sub>2</sub>/HD/D<sub>2</sub> and the H<sub>2</sub>/HD/D<sub>2</sub> rotational angular momentum  $\mathbf{j}$  couple to give the total angular momentum  $\lambda = \mathbf{l} + \mathbf{j}$ . Given the quantum numbers  $l$  and  $j$ ,  $\lambda$  can take values  $\lambda = l + j, l + j - 1, \dots, |l - j|$ , with the degeneracy of  $2\lambda + 1$ . The values of  $l$  are those allowed for the quantum number  $n$  of the isotropic 3D HO. The T-R states with the same quantum numbers  $n$  and  $j$  split into as many distinct levels (i.e., degenerate blocks) as there are different values of  $\lambda$ , each with the degeneracy  $2\lambda + 1$ .

With the help of the above model, we can explain the T-R level structure of H<sub>2</sub> (Tables I and II), HD (Tables III and IV), and D<sub>2</sub> (Figs. 5 and 6), on both PESs 1 and 2. Consider, for example, the six states of  $p$ -H<sub>2</sub> in Table I assigned as  $n=2, j=0$  ( $g_{n=2}^{\text{HO}}=6$ ). The allowed values of  $l$  are 0 and 2, and since  $j=0$ ,  $\lambda$  takes values 0 and 2 as well. Therefore, according to the model, the six  $n=2, j=0$  states should be split into a fivefold degenerate  $\lambda=2$  level and a nondegenerate  $\lambda=0$  level. Indeed, Table I shows two  $n=2, j=0$  levels,  $\lambda=2$  with the degeneracy  $g=5$ , and a nondegenerate

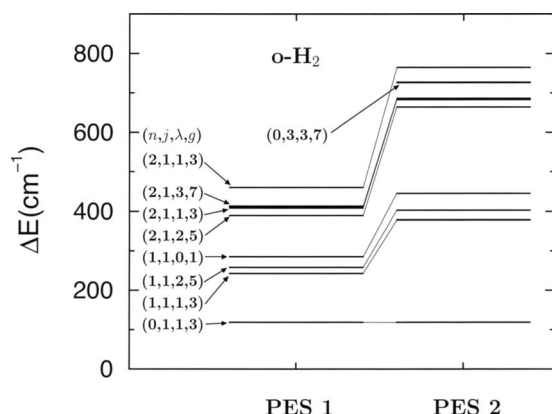


FIG. 3. Diagram of translation-rotation energy levels of  $o$ -H<sub>2</sub>@C<sub>60</sub> from the quantum 5D calculations on PES 1 and PES 2. The excitation energies  $\Delta E$  are relative to the ground-state energies on the two PESs. The quantum numbers  $(n, j, \lambda, g)$  are defined in the text.



TABLE III. Translation-rotation (T-R) energy levels of HD inside C<sub>60</sub>, from the quantum 5D calculations on PES 1 defined in the text. The excitation energies  $\Delta E$  (in cm<sup>-1</sup>) are relative to the ground-state energy  $E_0 = -931.822$  cm<sup>-1</sup>. Other symbols have the same meaning as in Table I. The numbers in the parentheses next to the  $c(j)$  values are those of the corresponding  $j$ ; the dominant  $j$  is in boldface. If its value is greater than 0.7, then it is the only one shown.

$n$	$j$	$l$	$\lambda$	$g$	$\Delta E$	$\langle R \rangle$	$c(j)$	
0	0	0	0	1	0.00	0.77	(0)0.964	
0	1	0	1	3	77.38	0.85	(0)0.354	(1)0.642
1	0	1	1	3	118.96	0.87	(0)0.591	(1)0.395
1	1	1	2	5	175.46	1.00	(0)0.305	(1)0.665
1	1	1	1	3	186.84	0.95	(1)0.977	
1	1	1	0	1	196.18	0.98	(0)0.467	(1)0.527
2	0	0,2	2	5	231.16	1.00	(0)0.553	(1)0.247
2	0	0,2	0	1	269.53	0.95	(0)0.486	(1)0.465
2	1	0,2	3	4	283.55	1.12	(0)0.263	(1)0.674
2	1	0,2	3	3	284.48	1.11	(0)0.262	(1)0.673
0	2	0	2	5	285.18	0.78	(2)0.791	
2	1	0,2	2	5	294.44	1.08	(1)0.912	
2	1	0,2	1	3	307.32	1.04	(1)0.857	
2	1	0,2	1	3	319.49	1.07	(0)0.384	(1)0.589
3	0	1,3	3	3	344.57	1.10	(0)0.489	(1)0.125
3	0	1,3	3	4	345.09	1.10	(0)0.489	(1)0.128
1	2	1	2	5	372.15	0.95	(2)0.931	
1	2	1	1	3	379.66	1.01	(0)0.314	(1)0.151
3	1	1,3	4	4	400.88	1.21	(0)0.223	(1)0.671
3	1	1,3	4	5	401.85	1.21	(0)0.223	(1)0.672
3	1	1,3	3	3	409.66	1.18	(1)0.840	
3	1	1,3	3	4	410.20	1.18	(1)0.839	
1	2	1	3	4	410.78	0.972	(0)0.149	(1)0.253
1	2	1	3	3	412.07	0.970	(0)0.150	(1)0.254
3	1	1,3	2	5	432.45	1.14	(1)0.814	
3	1	1,3	1	3	434.07	1.13	(1)0.815	

$\lambda=0$  level which is  $\sim 19$  cm<sup>-1</sup> higher in energy than the  $\lambda=2$  level on PES 2, and  $\sim 29$  cm<sup>-1</sup> on PES 1.

Another instructive example is provided by the ten states of  $p$ -H<sub>2</sub> in Table I assigned as  $n=3$ ,  $j=0$  ( $g_{n=3}^{\text{HO}}=10$ ). The  $l$  values allowed for  $n=3$  are 1 and 3. Given that  $j=0$ , these are also the values of  $\lambda$ . Consequently, we expect the  $n=3$ ,  $j=0$  states to appear as two distinct levels,  $\lambda=3$  with sevenfold degeneracy, and a threefold degenerate  $\lambda=1$  level. The latter is the last entry in Table I. But, the seven  $\lambda=3$  states, instead of being degenerate, are split into two closely spaced levels ( $\sim 0.3$  cm<sup>-1</sup> apart on both PESs), with fourfold and threefold degeneracies, respectively. As explained in paper I, this is a manifestation of the group-theoretical prediction by Judd,<sup>9</sup> who studied the energy levels of rare-earth ions in the crystal field of icosahedral  $I_h$  symmetry, that the seven (nine) states with  $\lambda=3(4)$  should be split into two sets of degenerate states, with dimensions (degeneracies) 3 and 4 for  $\lambda=3$ , and 4 and 5 for  $\lambda=4$ . The energy of the  $\lambda=1$  level is higher than that of the two with  $\lambda=3$  by  $\sim 30$  cm<sup>-1</sup> on PES 2 and by  $\sim 38$  cm<sup>-1</sup> on PES 1.

It is readily verified that every  $\lambda=3$  septet in Tables I–IV, on PES 1 and PES 2, is split into a pair of levels with  $g=3$  and 4, respectively, in accordance with group-theoretical prediction. The only example of  $\lambda=4$  states are those of HD on PES 1 in Table III, with  $n=3$ ,  $j=1$ ; the nine  $\lambda=4$  states are grouped in two levels with four- and fivefold degeneracies, separated by  $\sim 1$  cm<sup>-1</sup>. The “crystal field” splittings of the T-R levels are too small to be resolved on the

energy scale of Figs. 2–7. Therefore, for the  $\lambda=3,4$  levels shown in these figures, their degeneracies  $g$  are given as 7 and 9, respectively.

While the level splittings induced by the nonsphericity of C<sub>60</sub> are small, on the order of a wave number, the splittings between the levels with the same  $n, j$  values but differing in the quantum number  $\lambda$  are substantial and should be easily observable spectroscopically. They are generally in the range of 10–40 cm<sup>-1</sup> but can be as large as 78 (PES 2) and 47 cm<sup>-1</sup> (PES 1) between the  $\lambda=3$  and  $\lambda=1$  levels of  $o$ -H<sub>2</sub> with  $n=2$ ,  $j=1$  in Table II.

The success of the model which combines the isotropic 3D harmonic oscillator and the rigid rotor, with the coupling of the orbital and the rotational angular momenta of H<sub>2</sub> (D<sub>2</sub>, HD), in correlating and assigning the T-R energy level structure of H<sub>2</sub>/HD/D<sub>2</sub>@C<sub>60</sub> from the rigorous quantum 5D calculations, is remarkable. The ability to assign quantum numbers in a coupled multidimensional system is by no means trivial or guaranteed. It was not obvious *a priori* to us that the  $l$  values appropriate for the coupling with  $j$  to give  $\lambda$  would be those associated with the given quantum number  $n$  of the isotropic 3D HO. It is fortunate that this is true, because although the eigenvectors provide information about the quantum number  $j$  of every T-R state, through  $c(j)$ , they do not do this for  $l$ , since the Cartesian coordinates ( $x, y, z$ ) of the cm of H<sub>2</sub>/HD/D<sub>2</sub> are employed, not the spherical polar coordinates ( $|\mathbf{R}|, \Theta, \Phi$ ) mentioned in Sec. II. The translationally excited ( $j=0$ ) levels of H<sub>2</sub>/HD/D<sub>2</sub>@C<sub>60</sub> are actu-

TABLE IV. Translation-rotation (T-R) energy levels of HD inside  $C_{60}$ , from the quantum 5D calculations on PES 2 defined in the text. The excitation energies  $\Delta E$  (in  $\text{cm}^{-1}$ ) are relative to the ground-state energy  $E_0 = -1079.249 \text{ cm}^{-1}$ . Other symbols have the same meaning as in Table I. The numbers in the parentheses next to the  $c(j)$  values are those of the corresponding  $j$ ; the dominant  $j$  is in boldface. If its value is greater than 0.7, then it is the only one shown.

$n$	$j$	$l$	$\lambda$	$g$	$\Delta E$	$\langle R \rangle$	$c(j)$	
0	0	0	0	1	0.00	0.56	(0)0.904	
0	1	0	1	3	81.11	0.57	(1)0.827	
0	2	0	2	5	231.47	0.63	(1)0.421	(2)0.527
1	0	1	1	3	236.11	0.67	(0)0.731	
1	1	1	1	3	303.60	0.69	(1)0.930	
1	1	1	0	1	331.19	0.69	(0)0.363	(1)0.587
1	1	1	2	5	335.59	0.65	(0)0.247	(1)0.311
1	2	1	3	4	418.11	0.73	(1)0.320	(2)0.548
1	2	1	3	3	418.52	0.73	(1)0.318	(2)0.550
1	2	1	2	5	458.86	0.73	(1)0.312	(2)0.667
1	2	1	1	3	471.16	0.73	(1)0.469	(2)0.477
2	0	0,2	2	5	486.60	0.75	(0)0.549	(1)0.347
2	0	0,2	0	1	501.90	0.74	(0)0.572	(1)0.328
0	3	0	3	4	519.00	0.71	(0)0.162	(1)0.320
0	3	0	3	3	519.21	0.71	(0)0.161	(1)0.321
2	1	0,2	2	5	558.66	0.75	(1)0.601	(2)0.375
2	1	0,2	1	3	562.95	0.77	(1)0.730	(2)0.161
2	1	0,2	1	3	602.11	0.75	(0)0.378	(1)0.257
2?	1?	0,2?	3	4	620.16	0.67	(0)0.250	(2)0.242
2?	1?	0,2?	3	3	620.42	0.68	(0)0.256	(2)0.240

ally not harmonic since, as shown in Tables I, III, and IV and Fig. 5 and the discussion above about the  $n=2$ ,  $j=0$  and  $n=3$ ,  $j=0$  states, their energies depend not just on  $n$ , as in the isotropic 3D HO, but also quite strongly on  $l$  (i.e.,  $\lambda$ ).

There are instances when two T-R levels have the same  $n$ ,  $j$ , and  $\lambda$  quantum numbers. This happens, for example, when  $n=2$ ,  $j=1$ , and  $l=0,2$ . In this case,  $\lambda$  takes the values 3, 2, 1, and 1. Thus,  $\lambda=1$  appears twice, and consequently, there are two  $n=2$ ,  $j=1$  levels with  $\lambda=1$  (and  $l=0,2$ ). Two such levels of  $o\text{-H}_2$  are listed in Table II, at 683.78 and 765.32  $\text{cm}^{-1}$  on PES 2, or at 408.32 and 460.14  $\text{cm}^{-1}$  on PES 1. Another pair of levels of this type can be found for HD on PES 1 in Table III. This issue does not interfere with organizing the T-R level structure, but in order to label such pairs of levels uniquely, information about one additional quantum number, presumably  $l$ , is needed.

### B. How good a quantum number is $j$ for $\text{H}_2/\text{HD}/\text{D}_2$ @ $\text{C}_{60}$ ?

The knowledge of the quantum number  $j$  is central to the procedure for assigning the quantum numbers described in the previous section. So, how good a quantum number is  $j$ ? For the T-R states of  $p$ - and  $o\text{-H}_2$  in Tables I and II, on both PESs,  $j$  is a good quantum number, since the contribution of the dominant rotational basis function,  $j=0$  or 2 for  $p\text{-H}_2$  and  $j=1$  for  $o\text{-H}_2$ , is greater than  $\sim 0.7$ , indeed greater than 0.9 in most cases. The exception, noted in paper I, are two pairs of  $\lambda=3$  levels of  $o\text{-H}_2$  on PES 2 in Table II, the  $n=2$ ,  $j=1$  levels at 686.52 and 687.05  $\text{cm}^{-1}$ , and the  $n=0$ ,  $j=3$  levels at 726.79 and 727.73  $\text{cm}^{-1}$ , which probably interact; their  $c(1)$  and  $c(3)$  values, respectively, are in the range 0.62–0.64. Still, the assignment of these levels as  $j=1$  and  $j=3$  is meaningful and results in the complete assignment of the T-R

level structure in the energy range considered. Interestingly, the corresponding levels on PES 1 are rotationally highly pure. The most likely explanation for this observation is that in this case the corresponding pairs of  $\lambda=3$  levels with  $n=2$ ,  $j=1$  and  $n=0$ ,  $j=3$ , respectively, are  $\sim 300 \text{ cm}^{-1}$  apart, instead of  $\sim 40 \text{ cm}^{-1}$  on PES 2, so that their mixing is much weaker. We can say, in general, that for  $\text{H}_2$  and  $\text{D}_2$ , the  $j$  mixing, when it occurs, is due primarily to the accidental proximity of the T-R states having the same  $\lambda$  but different  $n, j$  values, which is of course very much PES dependent.

The heteronuclear isotopomer HD differs considerably in this respect from  $\text{H}_2$  and  $\text{D}_2$ . The majority of T-R levels of HD on PES 1 (Table III) and PES 2 (Table IV) exhibit strong mixing of two or three rotational basis functions. The dominant  $c(j)$ , whether  $j$  is 0, 1, 2, or 3, is often only slightly

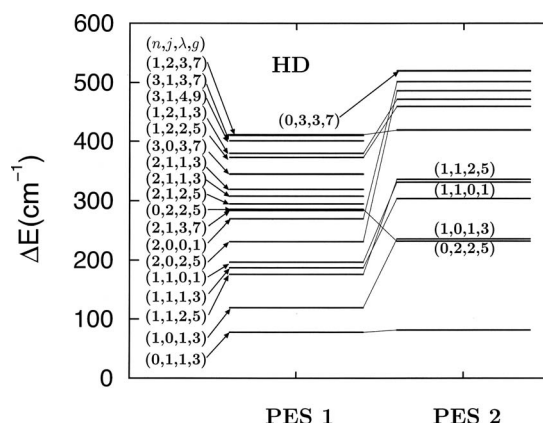


FIG. 4. Diagram of translation-rotation energy levels of HD@ $\text{C}_{60}$  from the quantum 5D calculations on PES 1 and PES 2. The excitation energies  $\Delta E$  are relative to the ground-state energies on the two PESs. The quantum numbers  $(n, j, \lambda, g)$  are defined in the text.

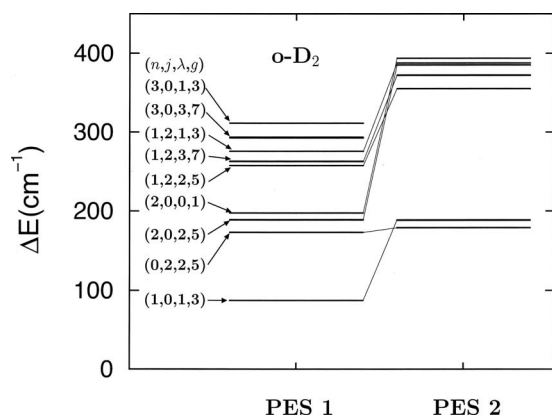


FIG. 5. Diagram of translation-rotation energy levels of *o*-D<sub>2</sub>@C<sub>60</sub> from the quantum 5D calculations on PES 1 and PES 2. The excitation energies  $\Delta E$  are relative to the ground-state energies on the two PESs. The quantum numbers  $(n,j,\lambda,g)$  are defined in the text.

greater than 0.5. In fact, for a number of levels on both PESs, the largest  $c(j)$  is smaller than 0.5, e.g., the  $n=2$ ,  $j=0$ ,  $\lambda=0$  level at 269.53 cm<sup>-1</sup> on PES 1 (Table III), with  $c(0)=0.486$ , followed by  $c(1)=0.465$ . Perhaps somewhat surprisingly, even for these levels, assigning the quantum number  $j$  according to the largest  $c(j)$  leads to  $\lambda$  values which account for the degeneracy patterns in the HD level structure.

This contrast between the homonuclear isotopomers H<sub>2</sub> and D<sub>2</sub> and the heteronuclear HD is not unique to C<sub>60</sub>, since we observed it also in another type of confinement, the small cage of the structure II clathrate hydrate. Our recent theoretical study<sup>21</sup> of this system found  $j$  to be a good quantum number for virtually all T-R states of H<sub>2</sub> and D<sub>2</sub> considered. In the case of HD, most T-R states showed considerable mixing of the  $j=0$  and  $j=1$  rotational basis functions.<sup>21</sup> HD owes this distinction, in both confining environments, to its mass anisotropy, which is not present in the two homonuclear isotopomers.

One manifestation, as well as an indicator, of the strong mixing between the basis functions with different  $j$ , is that the energies of the rotationally excited levels of HD in C<sub>60</sub> nominally assigned as  $j=1$ , 2, and 3, in the translational ground state  $n=0$ , deviate markedly from the corresponding

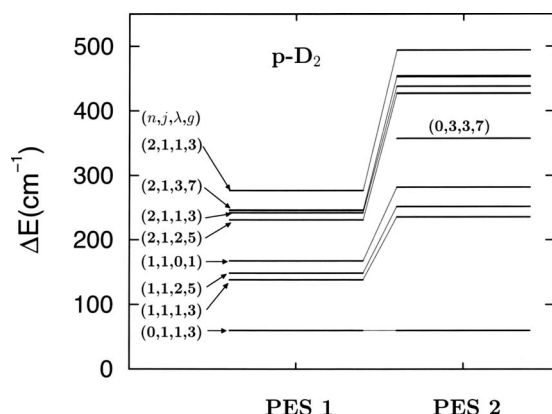


FIG. 6. Diagram of translation-rotation energy levels of *p*-D<sub>2</sub>@C<sub>60</sub> from the quantum 5D calculations on PES 1 and PES 2. The excitation energies  $\Delta E$  are relative to the ground-state energies on the two PESs. The quantum numbers  $(n,j,\lambda,g)$  are defined in the text.

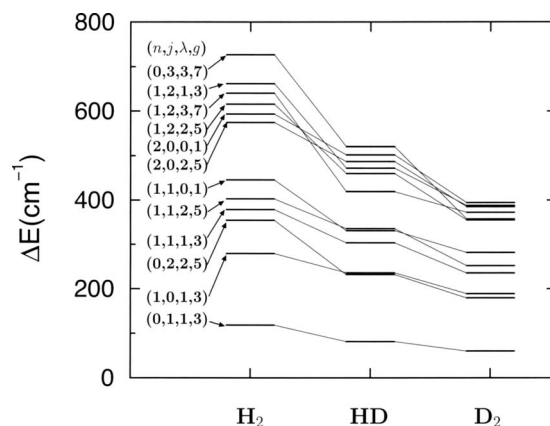


FIG. 7. Diagram of select translation-rotation energy levels of H<sub>2</sub>, HD, and D<sub>2</sub> in C<sub>60</sub> from the quantum 5D calculations on PES 2. The excitation energies  $\Delta E$  are relative to the ground-state energies of the isotopomers. The quantum numbers  $(n,j,\lambda,g)$  are defined in the text.

rotational levels of the freely rotating HD. Thus, on PES 2 (Table IV), the energies of the rotational levels in C<sub>60</sub> are 81.11 cm<sup>-1</sup> for  $j=1$ , 231.47 cm<sup>-1</sup> for  $j=2$ , and 519.00 cm<sup>-1</sup> for  $j=3$ , compared to 89.32 (2*B*), 267.97 (6*B*), and 535.94 cm<sup>-1</sup> (12*B*), respectively, for HD in the gas phase. In contrast the rotational levels of H<sub>2</sub> and D<sub>2</sub> in C<sub>60</sub> considered by us so far are generally within 1–2 cm<sup>-1</sup> of the gas-phase values. One of the rare exceptions is the pair of  $j=3$  levels of *o*-H<sub>2</sub> on PES 2 in Table II, discussed earlier; they lie at 726.79 and 727.73 cm<sup>-1</sup>, while in the gas phase the  $j=3$  level is at 12*B*=711.86 cm<sup>-1</sup>.

At higher excitation energies, the strongly mixed rotational character of the T-R levels of HD makes the quantum number assignment increasingly more difficult and ambiguous. To illustrate this, we turn to the group of the last five HD levels in Table IV. The first three, at 558.66, 562.95, and 602.11 cm<sup>-1</sup>, can be assigned with reasonable confidence as  $n=2$ ,  $j=1$ , and  $\lambda=2$ , 1, and 1, respectively. The number of  $n=2$ ,  $j=1$  ( $\lambda=3, 2, 1, 1$ ) states should be  $6 \times 3 = 18$ , and these three levels account for eleven states. It is necessary to identify two  $\lambda=3$  levels, with three- and fourfold degeneracies, which would bring the total to 18. The next two levels designated  $n=2?$ ,  $j=1?$ , at 620.16 and 620.42 cm<sup>-1</sup>, showing four- and threefold degeneracies, respectively, are the obvious candidates. However, their  $c(1)$  is very small, 0.058, and it is  $c(3)$  that has the largest value,  $\sim 0.43$ . In addition, the values of  $\langle R \rangle$  are unusually small for  $n=2$ . Thus, while these two levels clearly have  $\lambda=3$ , there is no basis for assigning them as  $n=2$ ,  $j=1$ , and hence the question marks.

What this means is that the model introduced in paper I and described in the previous section, which has proven highly successful for assigning the T-R levels of H<sub>2</sub> and D<sub>2</sub>, as well as the lower-lying levels of HD, begins to break down for HD at higher excitation energies. Ultimately, the only quantum number which remains good for HD appears to be  $\lambda$ , which can be established from the degeneracies of the levels and their splitting by the icosahedral environment of C<sub>60</sub>. The same must eventually happen also for H<sub>2</sub> and D<sub>2</sub> in C<sub>60</sub>, but the mass anisotropy of HD lowers the energy threshold.



It should be emphasized that the highly excited T-R levels of HD, H<sub>2</sub>, and D<sub>2</sub>, are calculated with the same high accuracy, and can be viewed and their properties analyzed, regardless of whether they can be assigned or not. The computational bound-state methodology described in Sec. II is rigorous and fully coupled, and does not rely on this or any other approximate model devised to understand and assign the T-R level structure.

### C. Dependence of the energy level structure on the potential energy surfaces and the isotopomers

PES 1 and PES 2 shown in Fig. 1 are very different in their well depths, shapes, and how tightly they confine the endohedral hydrogen molecule. The degree of confinement is visibly greater on PES 2, resulting in the frequency of the translational fundamental which is about a factor of 2 higher than on PES 1, for all three isotopomers. The translational fundamentals on PES 2 and PES 1 are 279.47 and 136.68 cm<sup>-1</sup>, respectively, for H<sub>2</sub>, 236.11 and 118.96 cm<sup>-1</sup> for HD, and 188.70 and 86.96 cm<sup>-1</sup> for D<sub>2</sub>.

With respect to the purely rotational excitations ( $n=0$ ), for H<sub>2</sub> and D<sub>2</sub>, their energies vary little on PESs 1 and 2,  $\sim 0.1$  cm<sup>-1</sup> for the  $j=1$  level and 3–5 cm<sup>-1</sup> for  $j=2$ . HD is again an exception. Its  $j=2$  level energies on PESs 1 and 2, 285.18 and 231.47 cm<sup>-1</sup>, differ by 53.7 cm<sup>-1</sup>; neither is close to the gas phase value of 267.97 cm<sup>-1</sup> [see the level designated (0,2,2,5) on PESs 1 and 2 in Fig. 4]. For the  $j=1$  level of HD, the difference is 3.7 cm<sup>-1</sup> (77.38 vs 81.11 cm<sup>-1</sup>). This large sensitivity of the rotational levels to the interaction potential is undoubtedly due to the unusually strong mixing of the basis functions with different  $j$  in the case of HD, discussed in the previous section.

T-R levels on PESs 1 and 2 with the same quantum numbers, which are translationally excited (with or without rotational excitation) differ greatly in energies and frequently, relative ordering. This is evident from Figs. 2–6, which display the T-R levels on the two PESs, and their relationships, for H<sub>2</sub>, HD, and D<sub>2</sub>. They reveal numerous instances of levels, or groups of levels, switching their places on PESs 1 and 2. In the case of  $p$ -H<sub>2</sub> (Fig. 2), the pair of translational excitations  $n=2$ ,  $j=0$ , with  $\lambda=0$  and 2, lies below the rotational excitation  $n=0$ ,  $j=2$  on PES 1, but is high above it in energy on PES 2. Another prominent exchange of places in going from PES 1 to PES 2 occurs between the translational excitations  $n=3$ ,  $j=0$ ,  $\lambda=1,3$  and the translation-rotation combinations  $n=1$ ,  $j=2$ ,  $\lambda=1,3$ . Additional examples can be found in Fig. 4 for HD, and Fig. 5 for  $o$ -D<sub>2</sub>.

PESs 1 and 2 give rise to T-R energy level structures which exhibit both quantitative and qualitative differences. Which of them is more accurate, closer to reality, in terms of the level patterns and actual excitation energies? In view of the simplicity of the two PESs and their purely empirical character, neither set of the computed T-R levels should be taken as, nor was it meant to be, a quantitative prediction. PESs 1 and 2 were used mainly to probe the sensitivity of the endohedral T-R dynamics to the interaction potentials and explore the energy level patterns which may arise. PES 2

appears to be in somewhat better agreement than PES 1 with the potential for H<sub>2</sub> inside C<sub>60</sub> shown in Fig. 1 of Ref. 22. However, that potential was calculated using the Hartree-Fock method, and its accuracy is questionable. Accurate anisotropic interaction potential for H<sub>2</sub>@C<sub>60</sub> is likely to emerge only through the interaction between high-level theory, quantum dynamics and electronic structure calculations, and spectroscopic measurements.

Finally, Fig. 7 displays in the middle the T-R levels of HD@C<sub>60</sub> on PES 2 and links them with their counterparts in  $p$ - and  $o$ -H<sub>2</sub>@C<sub>60</sub> and  $o$ - and  $p$ -D<sub>2</sub>@C<sub>60</sub>. This allows us to see the effects which the large differences in the masses and the rotational constants of the three isotopomers have on the calculated T-R level structure. Going from H<sub>2</sub> to HD and D<sub>2</sub>, the level energies decrease, as expected from the increasing masses and the decreasing rotational constants of the isotopomers. In addition, the ordering of many levels changes from one isotopomer to another, testifying to the pronounced isotopomer dependence of the level structure.

We conclude this section by presenting the ratios of the translational fundamentals calculated for the three isotopomers, denoted  $\omega_{H_2}$ ,  $\omega_{HD}$ , and  $\omega_{D_2}$ , and compare them to the corresponding ratios of the fundamentals for the isotropic 3D HO, shown in parentheses: (i) on PES 1,  $\omega_{H_2}/\omega_{HD}=1.149(1.155)$ ,  $\omega_{H_2}/\omega_{D_2}=1.572(1.414)$ ; (ii) on PES 2,  $\omega_{H_2}/\omega_{HD}=1.184(1.155)$ ,  $\omega_{H_2}/\omega_{D_2}=1.481(1.414)$ . The ratios of the translational fundamentals from the quantum 5D calculations are fairly close to those based on the model of the isotropic 3D HO.

## IV. CONCLUSIONS

We have performed fully coupled quantum 5D calculations of the T-R energy levels of H<sub>2</sub>, HD, and D<sub>2</sub> inside C<sub>60</sub>, using two 5D intermolecular PESs, designated PES 1 and 2, which differ substantially in their well depths and the extent to which they confine the endohedral hydrogen molecule. This work represented an extension of our initial investigation of the quantum dynamics of H<sub>2</sub>@C<sub>60</sub>,<sup>8</sup> and it utilized the same computational methodology. The objective of the present study was an in-depth exploration of the endohedral T-R dynamics, with the focus on its sensitivity to the properties of the PESs employed, and the impact of the large differences in the masses and the rotational constants of H<sub>2</sub>, HD, and D<sub>2</sub>.

Although having widely different excitation energies, the T-R levels of all three isotopomers, on both PESs, nevertheless display the same intriguing pattern of degeneracies found in our preliminary study of H<sub>2</sub> in C<sub>60</sub>.<sup>8</sup> Their level structure could be fully understood, organized, and assigned in terms of the physically motivated model developed by us earlier,<sup>8</sup> whose building blocks are the isotropic 3D harmonic oscillator and the rigid rotor, combined with the concept of coupling between the orbital and the rotational angular momenta of H<sub>2</sub>/HD/D<sub>2</sub>. This suggests that the physical picture and the understanding of the key factors governing the quantum T-R dynamics, which have emerged from our calculations in this and the previous paper,<sup>8</sup> are robust and not sensitive to the details of the interaction potentials.

The T-R levels of H<sub>2</sub>, HD, and D<sub>2</sub>, with the total angular momentum quantum number  $\lambda=3$  and 4, instead of being  $(2\lambda+1)$ -fold degenerate (such as those with  $\lambda=1$  and 2), appear as closely spaced pairs of levels with the degeneracies 3 and 4 for  $\lambda=3$ , and 4 and 5 for  $\lambda=4$ . This is a consequence of the icosahedral  $I_h$  environment of C<sub>60</sub>, which follows from the general group-theoretical argument.<sup>9</sup>

For H<sub>2</sub> and D<sub>2</sub>, both *ortho* and *para*,  $j$  was found to be a good quantum number on both PESs, with the contribution of the dominant rotational basis function greater than  $\sim 0.7$  (and in most cases  $>0.9$ ) for virtually all T-R states considered. HD is different in this respect. Most of its T-R levels exhibit strong mixing of two or more rotational basis functions; the contribution of the dominant rotational function is often only slightly larger than 0.5, and sometimes even smaller. The strongly mixed rotational character of the T-R levels of HD, unlike those of H<sub>2</sub> and D<sub>2</sub>, is probably due to the mass anisotropy of this isotopomer. One manifestation of the strong  $j$  mixing is the appreciable deviation of the energies of the rotational levels of HD in C<sub>60</sub>, on both PESs, from those of HD in the gas phase.

PES 2 confines the motions of the center of mass of the endohedral molecule much more than PES 1. As a result, the frequency of the translational fundamental on PES 2 is about a factor of 2 higher than on PES 1, for all three isotopomers. As for the purely rotational excitations, for H<sub>2</sub> and D<sub>2</sub>, their energies vary little on PESs 1 and 2,  $\sim 0.1$  cm<sup>-1</sup> for  $j=1$  and  $3-5$  cm<sup>-1</sup> for  $j=2$ . In contrast, for HD, the  $j=2$  level energy on PES 2 differs from that on PES 1 by  $\sim 54$  cm<sup>-1</sup>. This unusual sensitivity to the interaction potential is another consequence of the strong mixing of the rotational basis functions in the case of HD.

The T-R levels on PESs 1 and 2 with the same quantum numbers tend to differ substantially in the excitation energies and the energy gaps separating them. Their relative ordering on the two PESs is often different, especially if the levels involve translational excitation. Thus, the T-R level structures of H<sub>2</sub>, HD, and D<sub>2</sub> on PESs 1 and 2 show quantitative as well as qualitative differences. In view of the large uncertainties regarding the interaction potential for H<sub>2</sub> in C<sub>60</sub>, neither set of the calculated T-R levels is likely to represent a quantitative prediction. Instead, the T-R level structures on the two PESs provide (a) insight into the key features of the quantum dynamics of the confined hydrogen molecules and (b) patterns of energy levels, with their assignments, representative of what may be measured experimentally in the near future. We hope that accurate anisotropic interaction potential for H<sub>2</sub>@C<sub>60</sub> will emerge from the close interaction

between the multidimensional quantum dynamics and electronic structure calculations and sophisticated spectroscopic experiments.

## ACKNOWLEDGMENTS

Z.B. is grateful to the National Science Foundation for partial support of this research, through Grant No. CHE-0315508. The computational resources used in this work were funded in part by the NSF MRI Grant No. CHE-0420870. Acknowledgment is made to the donors of the American Chemical Society Petroleum Research Fund for partial support of this research. N.J.T. thanks the NSF for support of this research through Grant No. CHE-0717518.

- <sup>1</sup>K. Komatsu, M. Murata, and Y. Murata, *Science* **307**, 238 (2005).
- <sup>2</sup>M. Murata, Y. Murata, and K. Komatsu, *J. Am. Chem. Soc.* **128**, 8024 (2006).
- <sup>3</sup>Y. Rubin, T. Jarrosson, G. W. Wang, M. D. Bartberger, K. N. Houk, G. Schick, M. Saunders, and R. J. Cross, *Angew. Chem., Int. Ed.* **40**, 1543 (2001).
- <sup>4</sup>E. Sartori, M. Ruzzi, N. J. Turro, J. D. Decatur, D. C. Doetschman, R. G. Lawler, A. L. Buchachenko, Y. Murata, and K. Komatsu, *J. Am. Chem. Soc.* **128**, 14752 (2006).
- <sup>5</sup>M. Carravetta, A. Danquigny, S. Mamone *et al.*, *Phys. Chem. Chem. Phys.* **9**, 4879 (2007).
- <sup>6</sup>M. Carravetta, O. G. Johannessen, M. H. Leviitt, I. Heinmaa, R. Stern, A. Samoson, A. J. Horsewill, Y. Murata, and K. Komatsu, *J. Chem. Phys.* **124**, 104507 (2007).
- <sup>7</sup>J. Lopez-Gejo, A. A. Marti, M. Ruzzi, S. Jockusch, K. Komatsu, F. Tanabe, Y. Murata, and N. J. Turro, *J. Am. Chem. Soc.* **129**, 14554 (2007).
- <sup>8</sup>M. Xu, F. Sebastianelli, Z. Bačić, R. Lawler, and N. J. Turro, *J. Chem. Phys.* **128**, 011101 (2008).
- <sup>9</sup>B. R. Judd, *Proc. R. Soc. London, Ser. A* **241**, 122 (1957).
- <sup>10</sup>M. Xu, Y. Elmatad, F. Sebastianelli, J. W. Moskowitz, and Z. Bačić, *J. Phys. Chem. B* **110**, 24806 (2006).
- <sup>11</sup>F. Sebastianelli, M. Xu, Y. Elmatad, J. W. Moskowitz, and Z. Bačić, *J. Phys. Chem. C* **111**, 2497 (2007).
- <sup>12</sup>F. Sebastianelli, M. Xu, D. K. Kanan, and Z. Bačić, *J. Phys. Chem. A* **111**, 6115 (2007).
- <sup>13</sup>M. Xu, F. Sebastianelli, and Z. Bačić, *J. Phys. Chem. A* **111**, 12763 (2007).
- <sup>14</sup>K. Hedberg, L. Hedberg, D. S. Bethune, C. A. Brown, H. C. Dorn, R. D. Johnson, and M. de Vries, *Science* **254**, 410 (1991).
- <sup>15</sup>E. H. T. Olthof, A. van der Avoird, and P. E. S. Wormer, *J. Chem. Phys.* **104**, 832 (1996).
- <sup>16</sup>S. Liu, Z. Bačić, J. W. Moskowitz, and K. E. Schmidt, *J. Chem. Phys.* **103**, 1829 (1995).
- <sup>17</sup>Z. Bačić and J. C. Light, *Annu. Rev. Phys. Chem.* **40**, 469 (1989).
- <sup>18</sup>T. Lu, E. M. Goldfield, and S. K. Gray, *J. Phys. Chem. B* **110**, 1742 (2006).
- <sup>19</sup>S. J. V. Frankland and D. W. Brenner, *Chem. Phys. Lett.* **334**, 18 (2001).
- <sup>20</sup>A. D. Novaco and J. P. Wroblewski, *Phys. Rev. B* **39**, 11364 (1989).
- <sup>21</sup>M. Xu, F. Sebastianelli, and Z. Bačić, *J. Chem. Phys.* **128**, 244715 (2008).
- <sup>22</sup>R. J. Cross, *J. Phys. Chem. A* **105**, 6943 (2001).